B. Electrochem 4(6) June 1988, pp 551-557

POROUS IRON ELECTRODE FOR ALKALINE BATTERIES

G PARUTHIMAL KALAIGNAN, V S MURALIDHARAN and K I VASU
Central Electrochemical Research Institute, Karaikudi-623 006, INDIA

[Received: 1988 January; Accepted: 1988 April]

A method for characterising the sintered iron electrode based on triangular potential sweep voltammetry has been developed. The peak potential separation and (Qc/Qa) at zero sweep rates have been used as criteria of reversibility. The best composition based on using various iron powders, α- Fe_3O_4 and various additives has been recommended. Gasometric method to determine the self-discharge current and discharge studies of nickel-iron cell have been presented.

Key words: Iron electrode, T.P.S.V. method, alkaline batteries

INTRODUCTION

The use and development of iron electrodes have been receiving considerable attention from the period of invention of nickel-iron accumulator. Discharge studies in 5M KOH solutions revealed that the metal was oxidised to $Fe(OH)_2$ at the first discharge plateau and a mixture of FeOOH and Fe_3O_4 was obtained during second discharge [1-3]. Mossbauer Spectroscopy identified the phases is situ during the cyclic galvanostatic oxidation - reduction of iron. $Fe(OH)_2$ was found at the first anodic arrest and the second arrest was due to ß-FeOOH and unreacted $Fe(OH)_2$ [4,5]. The soluble species $HFeO_2^-$ and FeO_2^- in the formation of FeOOH and the effect of additives in 6M KOH on iron electrode behaviour have been discussed earlier [6,7]. The fast screening of additives to suppress the self-discharge of alkaline porous iron electrodes was carried out by the analysis of open-circuit potential decay curve [8]. The present study envisages a method of characterising the composition of sintered iron electrodes to ensure good reversibility, long cycle life and application of the same to discharge studies of assembled nickel-iron cell. The effect of additives on the reversibility and on the self-discharge of the iron electrodes is presented.

EXPERIMENTAL

Iron powders of different origins had been used and the properties of some of the powders used to prepare the electrodes are given in Table I. Electrolytic iron powder was reduced at 873K for

TABLE-I: Properties of powders used

S.No	Powder	Chemical composition	Apparent density (g/cc)	Tap density (g/cc)	Particle size (µm)	Specific surface area* (m^2/g)
A	Electrolytic iron powder	99% Fe, 0.001% Pb, 0.008% Zn, 0.001% As, 0.025% Mn, 0.005% Cu	2.84	3.08	$\leqslant$37	11.08
B	Water atomization iron powder (ASC 200)	>98% Fe, 0.01% C, 0.007% S, 0.007% P	2.8 - 3.0	-	92% < 60	18.52
C	Sponge iron powder (MH 300.25)	>98% Fe, 0.01% C, 0.007% S, 0.007% P	2.75 - 2.95	-	80% < 44 and 20% between 75 and 44	14.00
D	Synthetic black iron oxide (Fe_3O_4)	96.99% Fe_3O_4 Fe^{2+} = 44.55% Fe^{3+} = 25.73%	1.22	1.71	$\leqslant$37	38.72

* Quantasorb using liquid N_2

0256-1654/88/$ 3-50/

two hours in hydrogen atmosphere. Loose sintered electrodes were prepared from iron powder and the mixture of iron and iron oxide by using 10 mesh nickel grid of 0.1mm thick over which the powder was spread uniformly (area = 1.67 cm^2). Iron powder of different origins and Analar grade chemicals were used as additives. The electrodes were sintered at 1173K for one hour in hydrogen atmosphere. The amounts of Fe^{2+} ions in the Fe_3O_4 were estimated by usual methods [9]. The electrode was found to contain Fe = 89.46% Fe^{2+} = 6.68%, Fe^{3+} = 3.86%, in Fe + 15% Fe_3O_4 mixtures. Porous nickel electrodes were prepared from previously reduced INCO nickel 255 powder. Loose sintered electrodes were prepared by using nickel grids at 1123K for half-an-hour in hydrogen atmosphere. Electrochemical precipitation of active material in sintered electrode was made from nitrate bath. The electrodes were washed free of nitrate ion and used.

Detailed experimental set up for triangular potential sweep voltammetric (TPSV) method, gasometric method, discharge studies, and porosity measurements were described earlier [10]. Experiments in duplicate were carried out at 303 ± 0.01K. The 6M KOH solution containing 0.63M LiOH were deoxygenated by bubbling purified hydrogen for one hour. Potentials were measured against Hg/HgO reference electrode and no corrections were made for liquid junction potentials.

RESULTS AND DISCUSSION

The porous iron electrode was kept at -1.3V for five minutes, disconnected, shaken free of adsorbed hydrogen bubbles and polarised to -0.3V.

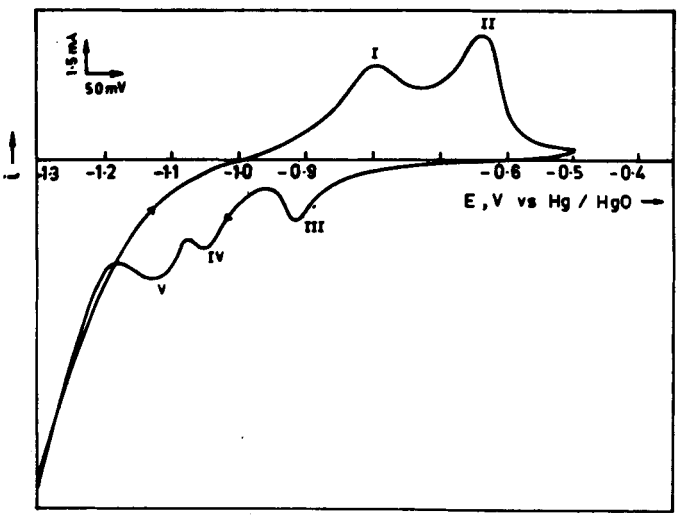

Fig.2: Typical cyclic voltammogram for electrolytic iron electrode with 8% nickel carbonate in deoxygenated 6.0M KOH + 0.63M LiOH solution Sweep rate = 0.5 mV/sec; $E_{\lambda,c}$ = -1·3 V; $E_{\lambda,a}$ = -0.5V

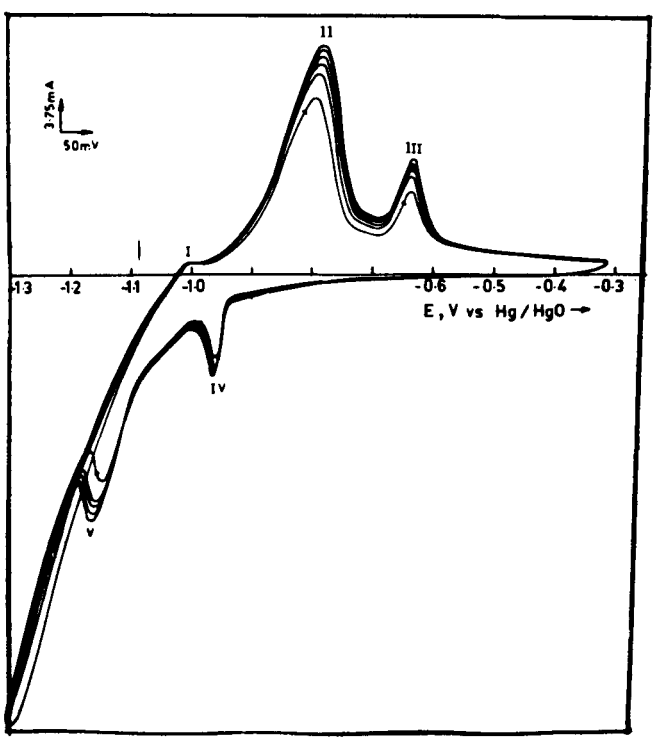

Fig.1: Typical voltammogram for electrolytic iron electrode (2 mm) in deoxygenated 6.0M KOH + 0.63M LiOH solution Sweep rate = 2 mV/sec; $E_{\lambda,c}$ = -1.3 V; $E_{\lambda,a}$ = -0.3 V

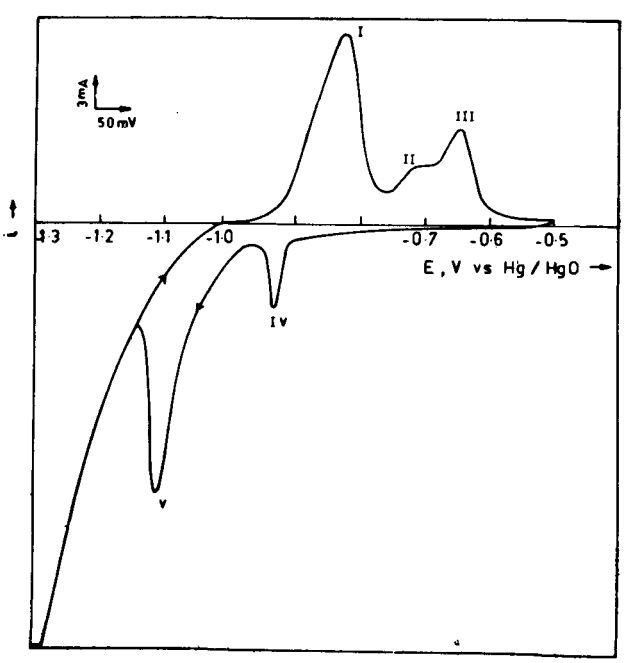

Fig.3: Typical cyclic votlammogram for electrolytic iron electrode with 10% cadmium oxide in deoxygenated 6.0M KOH+0.63M LiOH solution Sweep rate = 0.5mV/sec; $E_{\lambda,c}$ = 1.3 V; $E_{\lambda,a}$ = -0.5 V;

In 6M KOH solutions containing 0.63M LiOH, the electrochemical spectrum (Fig. 1) revealed in the forward scan a peak (I) at -950mV, peak (II) at -780mV and peak (III) at -625mV and in the reverse scan a cathodic peak (IV) at - 970mV followed by a cathodic peak (V) at -1170mV. On subsequent sweeping, the charge under peaks increased suggesting that the reactions are occurring in sequence. Increase of scan number shifted the peak potentials of (II) and (III) towards noble direction while the peak potentials of IV and V shifted towards more negative values suggesting mild reversibility of reactions with subsequent sweeping. Peak (I) is due to the conversion of Fe - $Fe(OH)_2$; peak (V) is due to the reduction of $Fe(OH)_2$ to Fe; and peak (III) may be due to the oxidation of $Fe(OH)_2$ to FeOOH. Fig.2 presents the electrochemical spectrum for electrolytic iron containing 8% $NiCO_3$. During forward scan two peaks appeared at -800mV (I) and -630mV (II) followed by three cathodic peaks on the reverse scan. The cathodic peaks appeared at -925 mV (III), -1050 mV(IV) and -1125 mV (V). The appearance of peak (IV) is due to the reduction of $HNiO_2$ or Ni $(OH)_2$ to nickel. In this potential region, reduction of $Fe(OH)_2$ to Fe is not possible.

The electrochemical behaviour of electrolytic iron electrode containing 10% CdO (Fig.3) has the following features. During forward scan, a peak appeared at -850mV (I) followed by a plateau at -750mV (II) and a peak at -650mV (III). On the reverse scan cathodic peaks appeared at -935mV (IV) and -1115mV(V). The appearance of plateau (II) is due to the formation of soluble divalent cadmium species. In the electrochemical spectrum for electrolytic iron containing 2% elemental sulphur (Fig.4), the forward scan has three peaks at -850mV (I), -780mV (II), and -480mV (III) followed by one cathodic peak on the reveerse scan at 1125mV (IV). There is no peak corresponding to the reduction of FeOOH to $Fe(OH)_2$. During sintering, the sulphide formed may hinder the formation of ferric iron, causing a shift of 160mV in the noble direction. The formed ferrous hydroxide and ferrous sulphide are reduced to iron at 1125mV. This is highly favourable for the deep discharge of iron electrode. Fig.5 presents the electrochemical spectrum for electrolytic iron containing 15% Fe_3O_4 and 2% thiourea. During the forward scan two peaks appeared at -675mV (I) and -550mV (II) followed by two cathodic peaks on the reverse scan at —1010mV (III) and — 1135mV (IV). In the presence of thiourea, the formation of $Fe(OH)_2$ is not readily favoured and also not easily oxidised to FeOOH. The appearance of a peak (III) at —1010mV is due to the reduction of Fe_3O_4 to $Fe(OH)_2$. At higher sweep rates, peak III and IV merge to give a single cathodic peak at — 1150mV. The presence of thiourea prevents the formation of FeOOH as in the case of addition of elemental sulphur to iron.

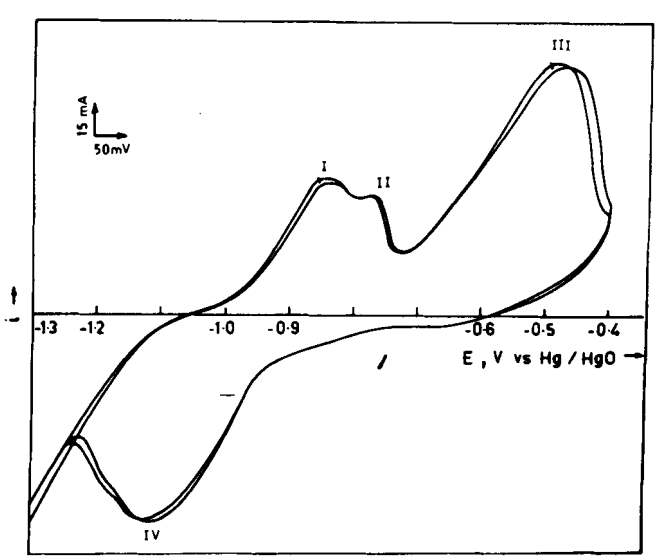

Fig.4: Typical cyclic voltammogram for electrolytic iron electrode with 2% elemental sulphur in deoxygenated 6.0M KOH + 0.63M LiOH solution Sweep rate = 1 mV/sec; $E_{\lambda,c}$ =-1.3V; $E_{\lambda,a}$ = =-0.4 V.

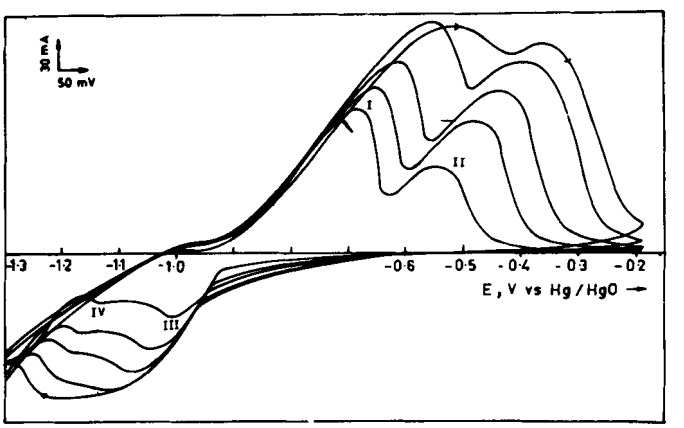

Fig.5: Typical cyclic voltammogram for electrolytic iron electrode with 15% Fe_3O_4 + 2% thiourea in deoxygenated 6.0M KOH + 0.63M LiOH solution with different sweep rates $E_{\lambda,c}$ = -1.3 V; $E_{\lambda,a}$ = -0.2 V.

An ideal reversible battery requires the electrodes of the second kind [11] i.e. a metal in contact with its sparingly soluble salt and solution saturated with the salt.

$$O_s + X + ne \rightleftharpoons R_s + Y \qquad \ldots (1)$$

Os and Rs are oxidant and reductant present in the solid phase and X and Y are species from the electrolyte.

In the case of iron electrode the charge storage reaction is

$$Fe(OH_2) + 2e \rightleftharpoons Fe + 2OH^- \qquad \ldots (2)$$

In TPSV studies (Fig.1) the appearance of anodic peak potential II and the cathodic peak potential V correspond to Fe/Fe(II) redox couple.

$$[\, E_p\,(II) - E_e \,] - [\, E_p\,(V) - E_e \,] = \Delta E_p \qquad \ldots (3)$$

This $\triangle$Ep is the measure of irreversibility. The more the value of E_p, the more the irreversibility of the electrode process. The fact that the electrode potential varies from -1.3V to -0.3V at different sweep rates corresponds to a situation of the discharge of a porous electrode at different rates. A slower sweep rate in TPSV study represents discharging a battery at low rates or connecting to a load of high impedance and following a single electrode potential with time. In other words, at low, ν iron electrode behaviour is being studied in a TPSV curve near reversible conditions. a high ν, will correspond to a situation of short circuiting a battery. Hence the extrapolation of peak potential separation ΔE_p to zero sweep rate will help in studying the electrode behaviour near reversible potential. An electrode which gives minimum ΔE_p at zero sweep rate will exhibit maximum reversibility and will be a good battery electrode. Similar procedure has been followed for

$$E_p\,(III) - E_p\,(IV) = \Delta E_p \qquad \ldots (4)$$

for Fe(II)/Fe(III) redox couple. The values of $\left(\frac{Qc}{Qa}\right)$ correspond to the charge associated with oxide reduction and oxide formation of Fe/Fe (II) and Fe(II)/Fe(III) couple. Even in solid electrodes, the values of $(\Delta E_p)_{\nu=0}$ for Fe/Fe(II) and Fe (II)/Fe(III) couples are 275 mV and 305 mV respectively. This amount of irreversibility is always present as the electrode surface is covered by oxide. An electrode which gives $(\Delta E_p)_{\nu=0}$ values closer to the solid electrode is considered to be the best electrode. As $\left(\frac{Qc}{Qa}\right)$ varies with ν, $\left(\frac{Qc}{Qa}\right)_{\nu=0}$ is taken as a measure of reversibility.

Table II presents the porosity and parameters derived from TPSV studies for different iron powders. All the iron powders exhibit more reversibility and values closer to solid electrode. Increase of electrode thickness decreases the porosity and reversibility. Though 1 mm thick electrode offers better reversibility compared with 2 mm electrodes, it has poor mechanical strength and hence 2 mm thick electrodes were used. Addition of iron oxide (α- Fe_3O_4) to various iron powders (Table III) increases the reversibility of sponge iron compared with other two iron powders. The best

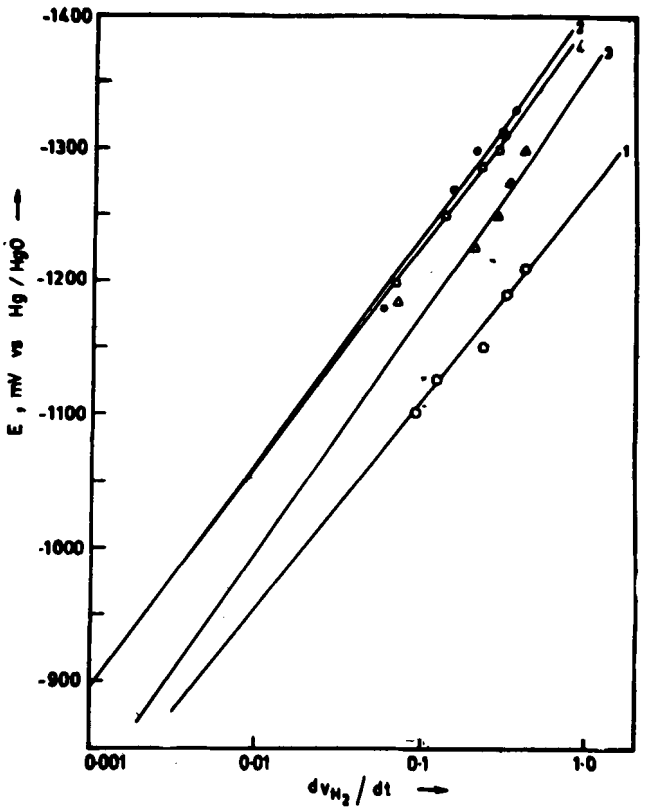

Fig.6: Applied potential 'E' vs log rate of hydrogen evolution

TABLE-II: Parameters derived from TPSV studies and porosity-effect of different iron powders and electrode thickness of electrolytic iron powder

Thickness	Nature of powder	$(\Delta E_p)_{\nu=0}$		$(Q_c/Q_a)_{\nu=0}$		Porosity
		Fe/Fe(II) couple (mV)	Fe (II)Fe (III)couple (mV)	Fe/Fe (II) couple	Fe(II) Fe (III)couple	
—	Solid electrode	275	305	0.74	0.89	—
1	A	312	288	0.96	1.00	70
2	A	326	278	0.74	0.81	60
3	A	454	375	0.72	0.65	55
2	B	410	380	0.86	0.77	61
2	C	400	360	0.65	0.66	60

was observed only in the case of electrolytic iron powder. α-Fe_3O_4 has been added to increase the ferrous and ferric content thereby incorporating more active material. The addition of Fe_3O_4 increases the irreversibility upto 15% but starts decreasing with further amounts of Fe_3O_4. Porosity decreases with increase of Fe_3O_4 up to 15% (Table III). Better sinterability and mechanical strength were observed with increase of Fe_3O_4 up to 15%. Addition of 10% CdO, 2% $NiCO_3$ and 1% elemental sulphur (Table IV) separately into electrolytic iron powder showed better reversibility. The value of $\left(\frac{Qc}{Qa}\right)_{\nu=0}$ is very small for the addition

TABLE-III: Parameters derived from TPSV studies and porosity-effect of various iron powders with iron oxide (D)

Electrode composition	$(\Delta E_p)_{\nu=0}$		$(Q_c/Q_a)_{\nu=0}$		Porosity %
	Fe/Fe (II) couple (mV)	Fe(II)/Fe(III)couple (mV)	Fe/Fe(II) couple	Fe(II)Fe(III)couple	
Solid electrode	275	305	0.74	0.89	—
A + 3% D	285	245	0.97	0.88	69
A + 5% D	365	300	0.77	0.59	71
A + 8% D	410	355	0.73	0.74	63
A + 15% D	408	300	0.91	0.84	61
A + 25% D	392	292	0.64	0.97	64
B + 10% D	343	328	0.78	0.90	59
B + 15% D	480	305	0.87	0.78	59
C + 10% D	458	374	0.52	0.78	59
C + 15% D	312	256	0.72	0.87	60

TABLE-IV: Parameters derived from TPSV studies and porosity-effect of additives to electrolytic iron powder

Additive %		$(\Delta E_p)_{\nu=0}$		$(Q_c/Q_a)_{\nu=0}$		Porosity %
		Fe/Fe(II) couple (mV)	Fe(II)/Fe(III)couple (mV)	Fe/Fe(II) couple	Fe(II)Fe(III)couple	
CdO	2	250	302	0.49	0.31	59
	4	255	282	0.66	0.56	61
	7	396	354	0.84	0.66	64
	10	260	272	0.88	0.81	67
	15	288	284	0.82	0.75	69
$NiCO_3$	2	248	248	0.89	0.74	60
	5	302	240	0.12	0.58	62
	8	310	250	0.41	0.57	65
	10	290	220	0.44	0.58	64
Elemental sulphur	0.25	268	—	0.81	—	59
	1	328	308	0.93	—	60
	2	264	—	0.92	—	65

TABLE-V: Parameters derived from TPSV studies and porosity-effect of different amounts of additives in a + 15% D

Additive %		$(\Delta E_p)_{\vartheta=0}$ Fe/Fe(II) couple (mV)	$(\Delta E_p)_{\vartheta=0}$ Fe(II)/Fe(III)couple (mV)	$(Q_c/Q_a)_{\vartheta=0}$ Fe/Fe(II) couple	$(Q_c/Q_a)_{\vartheta=0}$ Fe(II) Fe(III)couple	Porosity %
($NaBH_4$) Sodium borohydride	1.0	360	308	0.80	0.66	66
	2.0	356	328	0.76	0.92	68
	3.0	324	270	0.82	0.72	69
	4.0	274	268	0.88	0.50	69
(CH_3COOTl) Thallous acetate	1.0	288	274	0.70	0.83	66
	3.0	328	282	0.74	0.70	67
	4.0	286	280	0.72	0.72	70
Chromium metal powder	0.5	244	264	0.49	0.78	60
	1.0	314	295	0.72	0.75	60
	2.0	334	308	0.59	0.50	58
Thiourea	1.5	405	—	0.72	—	62
	2.0	386	405	0.77	—	65
FeS	0.1	438	280	0.65	0.80	60
	0.2	404	314	0.39	0.65	60
	0.3	326	312	0.85	0.82	64
	0.4	304	288	0.58	0.58	64

compared with the addition of CdO and sulphur. Addition of sodium borohydride, thallous acetate, chromium metal powder, thiourea and FeS to electrolytic iron powder containing 15% α-Fe_3O_4 were studied and Table V represents the parameters obtained from TPSV studies. Increase of sodium borohydride increases the porosity slightly and reversibility. 3% sodium borohydride gives more $\left(\frac{Qc}{Qa}\right)_{\vartheta=0}$ values. Increase of thallous acetate increases the porosity but has no effect on the reversibility. Increase of chromium metal powder content has no favourable effect on the reversibility and porosity. Increase of thiourea increases the porosity and reversibility. Addition of FeS decreases the $(Ep)_{=0}$ values while only 0.3% FeS has $\left(\frac{Qc}{QA}\right)_{\vartheta=0}$ close to 1.

TABLE-VI: Self discharge current of iron electrode in 6.0M KOH + 0.63M LiOH

Sl. No.	Electrode composition	Self discharge current (mA/g)
1	Electrolytic iron powder	0.80
2	Electrolytic iron powder + 15% Fe_3O_4	0.20
3	Electrolytic iron powder + 15% Fe_3O_4 + 10% CdO	0.52
4	Electrolytic iron powder + 15% Fe_3O_4 + 10% CdO + 0.3% FeS	0.18

Hydrogen evolution reaction is the parasitic reaction in the case of iron electrode. The electrode was polarised cathodically at five different potentials and the rate of hydrogen evolution was measured. Fig.6 presents a plot of potential vs rate of hydrogen evolution. The linear segment of the polarisation curves we extrapolated to open circuit potential to obtain self discharge current. Table VI presents the self discharge current of iron electrode for various electrode compositions. It may be seen the self discharge current is brought down to 25% and 22% by the addition of 15% Fe_3O_4 alone and 15% Fe_3O_4 + 10% CdO + 0.3% FeS respectively to the electrolytic iron powder.

Fig.7 shows the variation of electrode potential with time during discharge at different rates for a fully charged cell. The equilibrium potentials of Fe/Fe(II) and Fe(II)/Fe(III) couples are — 1.03V and — 0.715V respectively. The plateau observed in the discharge curves lies between —850mV to —885mV. This mixed potential arises due to the partial conversion of $Fe(OH)_2$ to FeOOH. With electrolytic iron powder containing 15% Fe_3O_4 + 10% CdO + 0.3% FeS the plateau potential is closer to the E_e of Fe/Fe(II) couple compared with other electrode compositions.

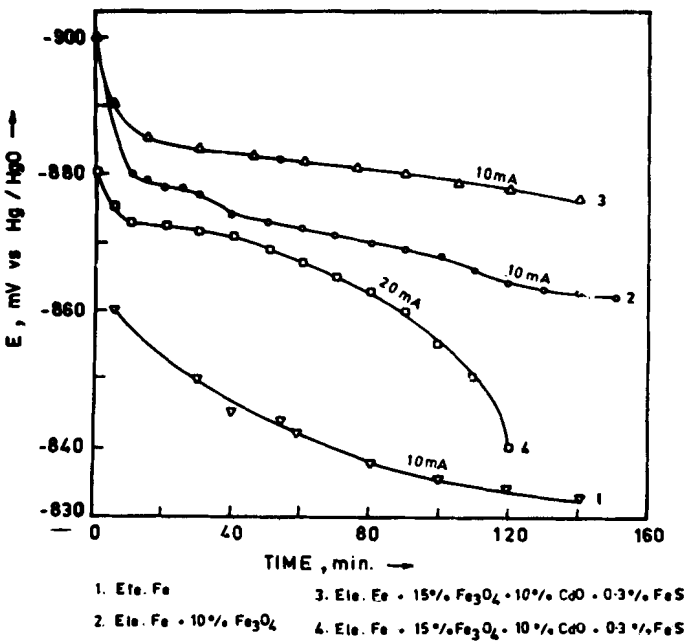

Fig.7: Variation of electrode potential with time during discharge at different rates

CONCLUSION

A method for characterising the sintered iron electrode material composition based on TPSV method has been developed. Addition of α-Fe_3O_4 and FeS to electrolytic iron powder improves charging efficiency and decreases self discharge current. Though CdO addition increases the self discharge current, it improves the reversibility. Studies on the TPSV, gasometric and discharge methods revealed that electrolytic iron powder containing 15% Fe_3O_4 + 10% CdO + 0.3% FeS to be an optimum composition for the fabrication of iron electrode.

REFERENCES

1. T K Teplurskaya, N N Fedorova and S A Rozentsveig, *Zh Fiz Khim,* **38** (1964) 2167

2. A J Salkind, C J Venuto and S U Falk, *J Electrochem Soc,* **111** (1964) 493

3. H G Silver and E Leaks,*ibid,* **117** (1970) 5

4. A M Pritchard and B J Mould, *Corros Sci,* **11** (1971) 1

5. Y Geronov, I Tomov and S Georgiev, *J Appl Electrochem,* **5** (1985) 675

6. V S Muralidharan and M Veerashanmugamani, *J Appl Electrochem,* **15** (1985) 675

7. G Paruthimal Kalaignan, V S Muralidharan and K I Vasu, *J Appl Electrochem* **17** (1987) 1083

8. K Vijaymohanan, A K Shukla and S Sathyanarayana, *J Power Sources,* **21** (1987) 53

9. I Vogel, *Text Book of Quantitative Inorganic Analysis* Fourth, Edition (Longman Group Ltd. London) (1978) p 354

10. G Paruthimal Kalaignan, V S Muralidharan, K I Vasu, *Trans SAEST,* **22** (1987) 67

11. S Sathyanarayana, *Trans SAEST,* **11** (1976) 19